

Received April 10, 2019, accepted April 22, 2019, date of publication April 30, 2019, date of current version May 31, 2019.

Digital Object Identifier 10.1109/ACCESS.2019.2914186

A Novel Auto-Focus Method for Image Processing Using Laser Triangulation

XIAOBO ZHANG¹, FUMIN FAN¹, MEHDI GHEISARI^{2,3}, AND GAUTAM SRIVASTAVA^{4,5}

¹Faculty of Automation, Guangdong University of Technology, Guangzhou 510006, China

²School of Computer Science and Cyber Engineering, Guangzhou University, Guangzhou 510006, China

³Young Researchers and Elites Club, Parand Branch, Islamic Azad University, Parand, Iran

⁴Department of Mathematics and Computer Science, Brandon University, Brandon, MB R7A 6A9, Canada

⁵Research Center for Interneural Computing, China Medical University, Taichung 40402, Taiwan

Corresponding authors: Mehdi Gheisari (mehdi.gheisari61@gmail.com) and Gautam Srivastava (srivastavag@brandonu.ca)

ABSTRACT Limitations of the pinhole method and astigmatic defocus detection have difficulties in determining the direction of defocus and a restricted linear correction range. Here, a distance-measuring approach based on the laser triangulation principle is proposed with a corresponding mathematical model to overcome these problems and to satisfy the requirements of an industrial thin-film transistor liquid-crystal display (TFT-LCD) inspection microscope system in active auto-focus applications. The approach combines infrared light at a wavelength of 808 nm with visible light. The light reflected from the surface of the object reaches a CCD camera and forms a spot via a set of optical devices. To control a PZT to achieve real-time auto-focusing, a Gaussian curve fitting method is used to process the spot information with the presented mathematical model giving the relationship between the detection value and the defocus value focus error signal (FES). The preliminary experiments with a 50× objective lens show that the measured values are consistent with the theoretical values, have good linearity and possess a focusing accuracy of 0.2 μm within ±30 μm of the focal plane. The analysis of the experimental results proves the feasibility of using this method in industrial applications. Compared with the traditional method of microscope focus correction, this method has the advantages of high accuracy, good linearity, and fast focus speed for the actual requirements of industrial inspection processes. This method has been applied to the circuit board component defect detection in our laboratory.

INDEX TERMS Optical images, laser triangulation, auto-focus, Gaussian curve fitting.

I. INTRODUCTION

Auto-focus technology is critical in automated vision inspection and industrial applications, such as the production of semiconductor components, TFT-LCD planes, IC chips, cell circuits, PCB inspection with the development of integrated circuits and computer technology [1].

In general, there are two different mechanisms for auto-focus implementation: passive control [2], [3], and active control [4], [5]. The passive auto-focus method is based on optimization of image sharpness metric or the image modulation transfer function. The continuous image sharpness analysis is reliable and robust in producing a clear image, but it is also time-consuming because it requires heavy data processing [6], [7]. To solve the problems of the passive auto-focus method, the active auto-focus method was designed [8], [9]. In the active auto-focus method, focusing is implemented by direct or indirect distance inspection. The examples of direct distance inspection are the infrared

distance method and ultrasonic ranging method [10]. The active auto-focus method does not require significant data processing, which overcomes the disadvantage of the passive auto-focus method.

This paper is organized as follows: We describe other related work in section 2. Section 3 is a discussion of our proposed design for an auto-focus microscope system based on geometric optics. In section 4, data preprocessing and Gaussian curve fitting for an FV (focus value) curve are introduced. In section 5, the experimental results and analysis are illustrated. Finally, in section 6, we present the conclusion.

II. RELATED WORKS

Past relevant research includes auto-focus technology in microscope systems [9]–[12], laser triangulation [13]–[16] and active auto-focus methods [4], [5], [8], [9]. The pinhole method [17], [18] and astigmatic defocus detection are the main active control auto-focus methods. However, these methods have difficulties in determining the direction of defocus and limitations in the range over which corrective adjustments are linear.

The associate editor coordinating the review of this manuscript and approving it for publication was Jun Wu.

In the past research, an active astigmatic auto-focus approach has been proposed, which is applied in compact disk or the head of digital versatile disk systems [8], [9]. Many different astigmatic optical algorithms have been proposed by researchers from different countries and applied to engineering of microscopes [19]–[21]. From the model of the astigmatic method [22], we know that the focus error signal (FES) and its derivative with respect to the distance from the sample object to the focal plane of the objective lens is not a real linear relationship, which limits widespread application of the method in microscopy [23].

For defocus detection, Ding *et al.* [24] presents a detection method of control points for the camera calibration that is robust to defocus. In calibration and measurement experiments, new marks are designed and control points are determined at intersects of the ridge curves. Experiments show that this method can obtain precise calibration and measurement results with images in a large defocus amount range. Hao *et al.* [10] used a laser, an adjacent prism focus and a four-quadrant photodetector to obtain the relationship curve between the FES and the defocus value. The experiment showed that the linear distance reached to $\pm 4\mu\text{m}$, and this method improves the ability of signal interference and has a higher stability. Lu *et al.* [22] and Hsu *et al.* [23] propose an astigmatic method to obtain the focus error and form a closed-loop to control a PZT that can realize fast and accurate auto-focusing in a laser direct writing system in certain scopes. This method solves the accuracy and speed limitations of [10]. In the astigmatic method, the relationship between defocus value and inspection value is not a linear relationship, but rather an approximate linear interval in certain scopes. For fast auto-focus, Wang *et al.* [25] proposes an optical defocus fitting model-based (ODFM) auto-focus scheme. Considering the basic optical defocus principle, the optical defocus fitting model is derived to approximate the potential-focus position. By this accurate modeling, the proposed auto-focus scheme can make the stepping motor approach the focal plane more accurately and rapidly. The proposed scheme can complete auto-focus within only 5 to 7 steps with good performance even under low-light condition.

In this paper, an elegant analytical formulation of the focus error signal is established based on geometric optics and may be used for designing different magnification objectives of the microscope. A new distance measuring method including a laser, CCD sensor and spectroscope in the microscope light path based on a laser triangulation principle is proposed in this paper. The purpose is to establish an auto-focus microscope system through different image focus positions (IFPs) [26] to determine the defocus direction and defocus value directly. Due to its fast focusing speed and good linearity, the design is applicable in FPD inspection, PCB inspection, bio-tech HCS and CMM machines, etc.

III. DESIGN OF THE AUTO-FOCUS MICROSCOPE SYSTEM

To realize automatic focusing, a photoelectric automatic focusing system based on laser triangulation is proposed [27].

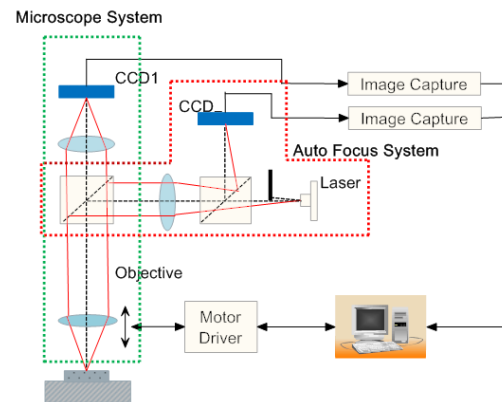


FIGURE 1. Design of the active auto-focus system.

As is shown in Figure.1, the auto-focus optical system of the microscope is composed of visible and infrared laser optics, including a laser, an IR cutoff filter, a beam splitter, a quartz wave-plate, a focusing mirror, a band-pass filter and CCD camera. To prevent the laser beam from affecting the image sensor of the microscope, an additional infrared 808nm laser source is combined with the visible light of laser beam. The upper portion of the combined beam is truncated when it passes through the IR cutoff filter, and when the beam passes through the optical components, such as the beam splitter, quartz wave-plate and focusing mirror, the lower portion of the beam becomes collimated light. Then, the laser beam passes through the objective lens and strikes the surface of the sample. The light reflected by the surface of the sample then returns to the path again, passes through a set of optical components and finally projects onto the CCD detector to be converted into a digital signal.

The computer can process digital signals after the steps as described thus far. The shape of the half-spot on the CCD detector changes according to the distance between the microscope objective lens and the surface of sample object. If the object is located at the front focal plane of the objective lens, the image plane on the CCD camera should be in focus, and a light spot should be detected. The distribution of this spot pattern depends on the defocus displacement.

Without considering the wavelength difference between the visible light and the infrared beam, they will focus at the same plane. When the objective lens is out of focus, the CCD will detect an upward or downward semicircle reflected by the sample if the image plane is in front or behind of the CCD detector plane. The radius of the semicircle will become smaller as the image plane moves closer to the CCD plane. Finally, it becomes a small point when the image plane (reflected by the object) is matched with the CCD detector plane which means that the focus procedure is completed. The defocus displacement can be determined according to distributions of the spot pattern (the shape, space and direction of the semicircle), as is shown in Figure.2. The shape of laser spot will be a point when the microscope is at the focal point, and the shape approaches an upward semicircle or downward

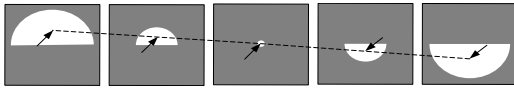


FIGURE 2. Different defocus amount measured by the spot image.

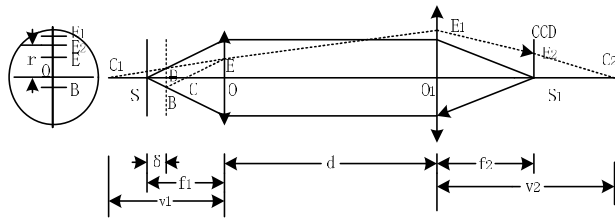


FIGURE 3. Principle of focus optical triangulation.

TABLE 1. The parameter definition for Figure.3.

Parameters	Definitions
$f1$	The focal length of the objective lens;
$f2$	The focal length of the focus lens;
d	The distance between the focus lens and the objective lens;
δ	The distance between the objective's focal point and sample surface;
r	The radius of the spot detected by the CCD;
D	The diameter of the collimated laser beam;

semicircle when the microscope approaches the limits of the working range.

The defocus direction can be obtained by analyzing the upward or downward semicircle on the CCD camera, and the defocus value can be calculated by measuring the pixel size of the semicircle. Using an exact mathematical relationship established by the laser triangulation principle, the motion controller controls the PZT to move the image plane to the expected plane (the focal plane) and completes the auto-focusing process rapidly.

The principle of a laser triangulation auto-focus system can simply be described as an optical system shown in Figure.3. The laser beam is focused on the sample surface and reflected back, converging to a point on the CCD detector because of the focusing lens as is shown in the figure with a solid vertical line. When the object is defocused by δ , the CCD sensor detects a semicircular spot due to changes in the reflected laser beam.

The parameters shown in Figure.3 are defined in Table 1:

The relationship between FES and semi-circular radius r detected by the CCD sensor based on geometric optics is analyzed as follows.

For a thin convex lens, the relationship among the object distance u , the lens focal distance f and the image distance v is given as follows according to the Gaussian lens law:

$$\frac{1}{f} = \frac{1}{u} + \frac{1}{v}$$

For the objective lens, the relationship is as follows:

$$\frac{1}{f_1} = \frac{1}{f_1 - 2\delta} + \frac{1}{v_1} \quad (1)$$

For the focus lens, the relationship by the Gaussian lens law is as follows:

$$\frac{1}{f_2} = \frac{1}{d - v_1} + \frac{1}{v_2} \quad (2)$$

The distance values of EO , E_1O_1 and R can be obtained according to trigonometric theory as follows:

$$EO = \frac{(f_1 - 2\delta) \cdot \delta \cdot \tan \theta}{\delta} \quad (3)$$

$$E_1O_1 = \frac{(u_1 + d) \cdot EO}{u_1} \quad (4)$$

$$R = \frac{(V_2 - f_2)}{v_2} \cdot E_1O_1 \quad (5)$$

$$r = R * P_z \quad (6)$$

Substituting (1), (2), (3), (4) and (5) into (6), the result is the elegant formulation of the FES:

$$FES = e_N(r) = \delta = \frac{f_1 \cdot P_z}{2f_2 \tan \theta} \cdot r \quad (7)$$

In (7), $\tan \theta$ is a constant which equals $D/(2 * f1)$, P_z is the pixel size, and $f1$ and $f2$ are the focal lengths of the objective lens and focusing lens, respectively. It can be concluded that there is a linear relationship between the FES and r from formulation (7) and that the line crosses through the coordinate origin. The linear slope (i.e., sensitivity) correlates with some optical parameters such as the focal lengths of objective lens and focus lens, the NA of the objective lens and the CCD pixel size, P_z , etc. The FES value can be estimated immediately from the radius r .

IV. FAST AUTO-FOCUS ALGORITHM FOR A MICROSCOPE SYSTEM

A. DATA PREPROCESSING

The color image captured by the CCD sensor is composed of red, green and blue channels. To simplify the image processing, an RGB to GRAY color space transformation is taken before information processing. The transformation formula is shown as follows:

$$GRAY = [0.299 \quad 0.587 \quad 0.144] * \begin{bmatrix} R \\ G \\ B \end{bmatrix} \quad (8)$$

To analyze the image data exactly, the gray value can be expressed as I :

$$I_{(j,i)} = GRAY(j, i)/255 \quad (9)$$

In (9), $GRAY(j,i)$ is the gray level intensity of pixel (j, i).

The value I_m (the average gray value) and maximum value I_{max} (the maximum gray value) that are used as parameters for the FV (Focus Value) can be determined from the columns of the image data (1 pixel to 640 pixels region).

To eliminate the effect of ghosting on the accurate positioning of the spot center, the smooth curve FV is defined as follows:

$$FV = 0.6I_m + 0.4I_{max} \quad (10)$$

$$I(i)_{\max} = \max\{I_{(j,i)}\}, \quad 1 \leq j \leq N \quad (11)$$

$$I(i)_m = \frac{1}{N} \sum_{j=1}^{j=N} I(j, i) \quad (12)$$

The weight factors for every parameter could be adjusted for TFT-LCD plane inspection. Figure.4 (a) shows the image when the object is defocused and Figure.4 (b) shows the FV curve from (10).

B. GAUSSIAN CURVE FITTING

In theory, the image should have enough features to produce a smooth FV curve. Assuming that the FV follows a Gaussian distribution, then the center of the Gaussian curve is fit to FV distribution. In this auto-focus system, Gaussian curve fitting is used to calculate the in-focus position to detect the defocus value and defocus direction. Due to fewer images required for auto-focusing compared with the traditional method, the Gaussian curve fitting method has the advantages of high accuracy, good linearity and fast focus speed.

The curve of the Gaussian function is as follows:

$$y(x) = ae^{-(x-u)^2/\delta^2} \quad (13)$$

The expected value of function $y(x)$ and δ should have minimum errors.

$$\delta = \min \sum [y - \hat{y}] \quad (14)$$

To obtain $y(x)$, u and δ are calculated by a residual sum of squares method (RSSM). The partial equation of u and δ could be determined first to obtain a matrix Z_0 , composed of f_u and f_δ .

$$\begin{cases} f_u = \frac{\partial f}{\partial u} = \frac{e^{-(x-u)^2/\delta^2}(x-u)}{e^3} \\ f_\delta = \frac{\partial f}{\partial \delta} = \frac{e^{-(x-u)^2/\delta^2}(x-u)^2}{e^3} \end{cases} \quad (15)$$

$$Z_0 = \begin{bmatrix} f_{u1} & f_{\delta 1} \\ \cdot & \cdot \\ f_{ui} & \cdot \cdot f_{\delta i} \\ \cdot & \cdot \\ f_{um} & f_{\delta m} \end{bmatrix} \quad (16)$$

Letting the initial value of u equal the center of mass of the image in the horizontal direction and δ equal the search region, the matrix D (a stokes vector of error y) can be determined by the following equation.

$$D = \begin{bmatrix} y_1 - \hat{y}_1 \\ y_2 - \hat{y}_2 \\ \cdot \\ \cdot \\ y_i - \hat{y}_i \end{bmatrix} \quad (17)$$

The modified matrix ΔA , is derived from (18) and (19) for new u and δ , namely \hat{u} and $\hat{\delta}$. ΔA is the intermediate result for u and δ .

$$Z_i^T Z_i \Delta A = A_i^T D \quad (18)$$

$$\begin{bmatrix} \hat{u} \\ \hat{\delta} \end{bmatrix} = \begin{bmatrix} u \\ \delta \end{bmatrix} + \Delta A \quad (19)$$

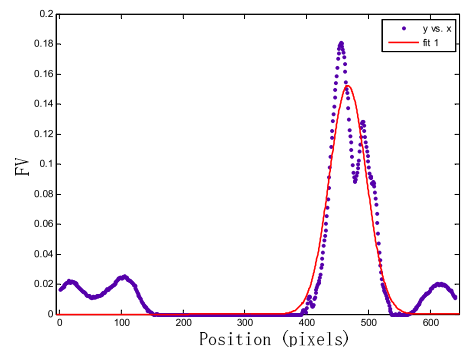
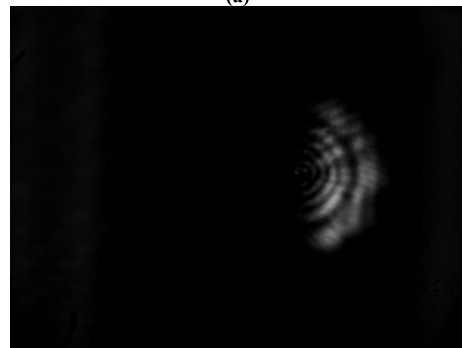
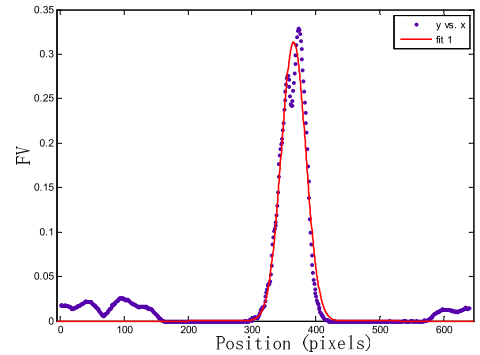
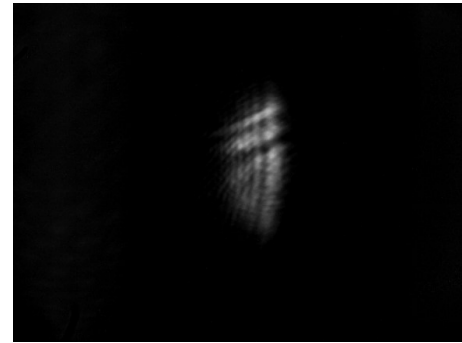


FIGURE 4. (a) Source image. (b) FV curve result.

These steps are repeated until ΔA is small enough so that $y(x)$ could be a fitting curve, and IFP u and δ can also be achieved. Figure.4 shows the result.

V. EXPERIMENTS AND ANALYSIS

A. HARDWARE DESIGN

In this experiment, the structure of the astigmatic auto-focus microscope system is shown in Figure.5, which comprises a

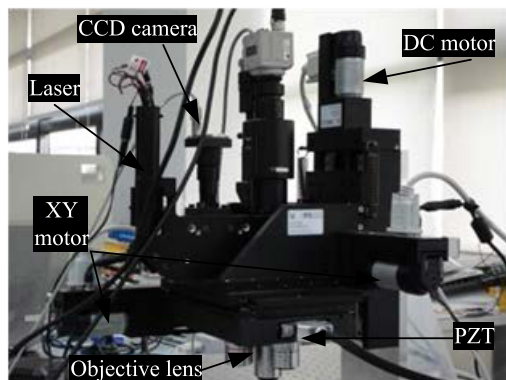


FIGURE 5. Structure of the astigmatic auto-focus microscope system.

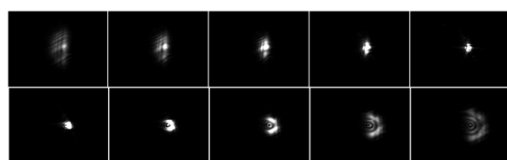


FIGURE 6. Different defocus amounts collected by the spot image.

laser source, beam splitters, PZT motor, DC motor, computer and an image sensor (CCD).

The wavelength of the laser emitter is 808nm. To prevent the laser beam from affecting the image sensor of the microscope, the Edmund L53-710 filter film is added into the microscope system with transmission, T , of more than 85% for visible light and T of less than 10% for light in the 740-1200nm wavelength range. The focusing lens has f_2 (150mm), the 50 \times objective lens has f_1 (4mm), the CCD camera's resolving power is 752 μm *480 μm and the pixel size P_z is 6 μm *6 μm . The sample object is a TFT-LCD plate with an integrated circuit inside and a surface thickness of 2.5mm.

Figure.6 is a set of pictures captured by the CCD detection screen of the spots in different defocus cases. The radius and direction of the semicircular spot will change when the distance between the object and objective lens changes. This result is consistent with the theoretical analysis.

Figure.7 shows the linear relationship between the focus error with the in-focus position and the IFP. When the IFP is at the position of 400 pixels in the image, the microscope system has completed focusing. The radius of the optical spot will be smallest when δ is at the minimum value of 20, as shown in Figure.7 (b). In Figure.7 (a), the region of linearity is from -30 μm to +30 μm , which means that if we had detected the IFP value, the distance from the in-focus position could be estimated immediately.

B. ANALYSIS OF EXPERIMENTAL RESULTS

The auto-focus experiment is divided into two parts: one is above the focal plane (TFP), and the other is below the focal plane. The experiment was repeatedly executed 16 times with raw data. Table 2 shows the experimental results.

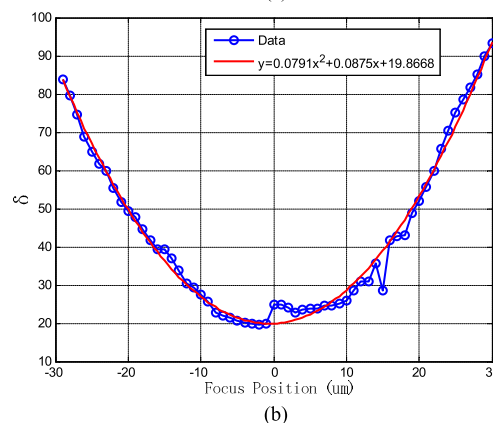
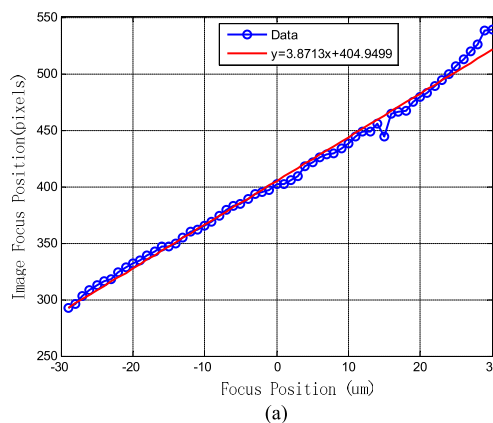


FIGURE 7. The relationship between the focus error with in-focus position and IFP/δ. (a) The relationship between in-focus position and IFP. (b) The relationship between in-focus position and δ.

TABLE 2. Experimental results of auto-focusing.

No.	Start place(μm)	Focus place(μm)	Time(s)
1	59.783	50.371	0.259
2	89.026	50.464	0.259
3	89.019	50.411	0.263
4	89.030	50.743	0.263
5	89.018	50.711	0.259
6	89.001	50.508	0.261
7	89.034	50.627	0.265
8	89.032	50.423	0.260
9	11.061	50.514	0.251
10	11.063	50.575	0.251
11	11.081	50.384	0.263
12	11.075	50.643	0.264
13	11.062	50.489	0.253
14	11.059	50.334	0.252
15	11.062	50.592	0.252
16	11.090	50.462	0.259

Table 2 shows that there is no statistical difference between the estimated value of the focus position by the IFP and the actual value, regardless of the initial position.

TABLE 3. Auto-focus experimental results.

Microscope objective	MSD	Ave Time	linear Range	DOF
50x	0.015 μ m	0.26s	+30 μ m	0.5 μ m

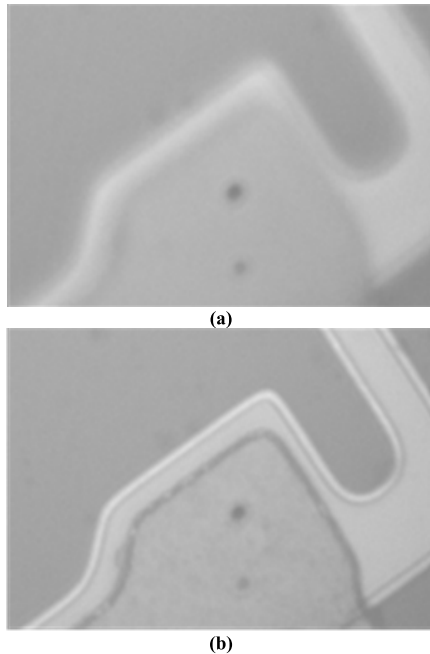


FIGURE 8. Sample plate images defocused and focused. (a) Image defocused. (b) Image focused.

The modified standard deviations (MSD) associated with the 16 sequences are summarized with the following definition.

$$MSD = \sqrt{\frac{\sum_{i=1}^N (m_p - \hat{m}_a)^2}{N - 1}} \quad (20)$$

In this definition, \hat{m}_a and m_p are the estimated value and actual value of the focus positions, and N is the number of experiments. Experimental results show that for the case of a 50 \times microscope objective, the focus MSD is 0.015, focusing time is less than 0.3s and the values are linear over a range from $-30\mu\text{m}$ to $+30\mu\text{m}$, as is shown in Table 3.

The TFT-LCD sample plate images defocused and focused are shown in Figure.8 (a) and Figure.8 (b).

VI. CONCLUSION

In our laboratory, we have developed a laser triangulation auto-focus system for use in microscopy, and this method has been used for circuit board defect detection in industry. An elegant analytical formulation of the focus error signal (FES) was established based on geometric optics and could be used to design different magnification objectives of the microscope. We propose a new method including a laser, CCD sensor and spectroscope in the microscope visible light path based on the principle of laser triangulation. The new auto-focus approach uses a combination of lenses and laser triangulation for probing the precise focus value and focus

direction in an industrial auto-focus system. For accurate analysis of the relationship between the spot information system and the defocus value, Gaussian curve fitting is introduced to the extraction algorithm.

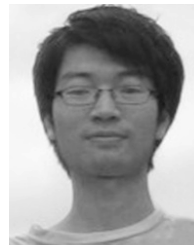
The experimental results show that a 50 \times objective lens has a focusing accuracy of $0.2\mu\text{m}$ and better linearity than traditional method at the focal plane of $\pm 30\mu\text{m}$ with the parameters of $NA = 0.55$ and $f1 = 4\text{mm}$. The algorithm proposed in this paper is consistent with the theoretical prediction. Compared with the traditional method of active focusing, this method can not only control the focus value and direction accurately but can also calculate a defocus value and spot radius by Gaussian curve fitting with excellent linearity. The system can find the in-focus position quickly without the continuous searching required by other search algorithms. In this research, the auto-focus system can find the focus position within a few seconds.

According to the experimental results, it can be concluded that the image focus position is estimated rapidly and accurately by the system, which means the method could be applied to LCD-TFT, FPD inspection, PCB inspection, and biomedical automatic machine assembly, etc. The inspection method for the defocus value and direction is also applicable for laser direct writing, confocal scanning and so on.

REFERENCES

- [1] H. Dogan, S. Ayas, and M. Ekinici, "Auto-focusing with multi focus color image fusion based on curvelet transform on microscopic imaging," in *Proc. 3rd Int. Conf. Elect. Electron. Eng.*, Istanbul, Turkey, 2016, pp. 253–258.
- [2] C.-Y. Chen, R.-C. Hwang, and Y.-J. Chen, "A passive auto-focus camera control system," *Appl. Soft Comput.*, vol. 10, no. 1, pp. 296–303, Jan. 2010.
- [3] G. Mark, R. Mohammad, and K. Nasser, "Performance metrics for passive auto-focus search algorithms in digital and smart-phone cameras," *J. Imag. Sci. Technol.*, vol. 55, no. 1, p. 10507, 2011.
- [4] D. Hannifin, J. N. Alpern, and J. Alpern, "Feature focus: Active directory," in *Microsoft Windows Server 2008 R2 Administrator's Reference: The Administrator's Essential Reference*. Syngress, 2010, pp. 141–248.
- [5] L. A. Bitzer, M. Elagin, M. P. Semtsiv, W. T. Masselink, N. Benson, and R. Schmechel, "Scanning light stimulation system with active focus correction at μm resolution for PV applications," *IEEE J. Photovolt.*, vol. 5, no. 2, pp. 627–632, Mar. 2015.
- [6] M. M. M. Kia, J. A. Alzubi, M. Gheisari, X. Zhang, M. Rahimi, and Y. Qin, "A novel method for recognition of persian alphabet by using fuzzy neural network," *IEEE Access*, vol. 6, pp. 77265–77271, 2018.
- [7] K. Strzecha, T. Koszmider, D. Zarebski, and W. Łobodziński, "Passive auto-focus algorithm for correcting image distortions caused by gas flow in high-temperature measurements of surface phenomena," *Image Process. Commun.*, vol. 17, no. 4, pp. 379–384, 2012.
- [8] P. N. Hedde and E. Gratton, "Active focus stabilization for upright selective plane illumination microscopy," *Opt. Express*, vol. 23, no. 11, pp. 14707–14714, 2015.
- [9] H.-C. Chang, T.-M. Shih, N. Z. Chen, and N.-W. Pu, "A microscope system based on bevel-axial method auto-focus," *Opt. Lasers Eng.*, vol. 47, no. 5, pp. 547–551, 2009.
- [10] X. Hao, J. Ren, and Z. Zou, "Design of focus error detection system based on critical angle method," *Opt. Precis. Eng.*, vol. 17, no. 3, pp. 537–541, 2009.
- [11] G. Saini, R. O. Panicker, B. Soman, and J. Rajan, "A comparative study of different auto-focus methods for Mycobacterium tuberculosis detection from brightfield microscopic images," in *Proc. IEEE Distrib. Comput., VLSI, Elect. Circuits Robot. (DISCOVER)*, Mangalore, India, Aug. 2016, pp. 95–100.

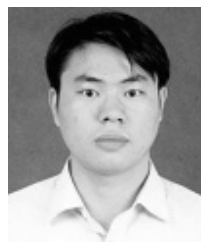
- [12] P. Guojin, Y. Zhenming, and Y. Jianhai, "Auto-focus windows selection algorithm for optical microscope," *J. Appl. Opt.*, vol. 36, no. 4, pp. 550–558, 2015.
- [13] Y. Selami, W. Tao, Q. Gao, H. Yang, and H. Zhao, "A scheme for enhancing precision in 3-dimensional positioning for non-contact measurement systems based on laser triangulation," *Sensors*, vol. 18, no. 2, p. 504, 2018.
- [14] S.-Q. Wu, B. Shen, J.-H. Wang, D.-T. Zheng, and J. Fleischer, "Super-resolution algorithm for laser triangulation measurement," *Lasers Eng.*, vol. 38, nos. 3–6, pp. 385–395, 2017.
- [15] S. Xiang, F. Pan, K. Xiang, and X. Wang, "Melt level measurement for the CZ crystal growth using an improved laser triangulation system," *Measurement*, vol. 103, pp. 27–35, Jun. 2017.
- [16] H. Wang, L. Hui, and J. Zhang, "Research on spot of CCD subdivided locating methods in laser triangulation displacement measurement," *Proc. SPIE*, vol. 10256, Feb. 2017, Art. no. 102562U.
- [17] D. Wen-Liang and T. Xiao-Lin, "An automatic image registration evaluation model on dense feature points by pinhole camera simulation," in *Proc. IEEE Int. Conf. Image Process.*, Beijing, China, 2017, pp. 2259–2263.
- [18] D. Duerr, "Lifting lug with pinhole bushing," *Pract. Periodical Struct. Des. Construct.*, vol. 23, no. 2, 2018, Art. no. 04018008.
- [19] L. Zhang, Y. Li, J. Wang, and Y. Liu, "Research on adaptive optics image restoration algorithm based on improved joint maximum a posteriori method," *Photonic Sensors*, vol. 8, no. 1, pp. 22–28, 2018.
- [20] J. G. Davis and W. S. Truscott, "Multiple reflection suppression algorithm for terahertz quasi-optic systems," *Electron. Lett.*, vol. 46, no. 1, pp. 52–54, 2010.
- [21] R. Wu, J. Sasián, and R. Liang, "Algorithm for designing free-form imaging optics with nonrational B-spline surfaces," *Appl. Opt.*, vol. 56, no. 9, pp. 2517–2522, 2017.
- [22] Y. Lu, X. Zhang, and H. Li, "A simplified focusing and astigmatism correction method for a scanning electron microscope," *AIP Adv.*, vol. 8, no. 1, 2018, Art. no. 015124.
- [23] W.-Y. Hsu et al., "Development of the fast astigmatic auto focus microscope system," *Meas. Sci. Technol.*, vol. 20, no. 4, pp. 45902–45910, 2009.
- [24] W. Ding, X. Liu, D. Xu, D. Zhang, and Z. Zhang, "A robust detection method of control points for calibration and measurement with defocused images," *IEEE Trans. Instrum. Meas.*, vol. 66, no. 10, pp. 2725–2735, Oct. 2017.
- [25] Y. Wang, H. Feng, Z. Xu, Q. Li, Y. Chen, and M. Cen, "Fast auto-focus scheme based on optical defocus fitting model," *J. Mod. Opt.*, vol. 65, no. 7, pp. 858–868, 2018.
- [26] F. Orioux, E. Sepulveda, V. Lorette, B. Dubertret, and J.-C. Olivo-Marin, "Bayesian estimation for optimized structured illumination microscopy," *IEEE Trans. Image Process.*, vol. 21, no. 2, pp. 601–614, Feb. 2012.
- [27] F. M. Fan, L. L. Cheng, X. F. Wang, and J. H. Pan, "A new type of high-speed automatic focusing system," *Opto-Electron. Eng.*, vol. 37, no. 5, pp. 127–132, 2010.



FUMIN FAN was born in 1984. He received the master's degree from the Faculty of Automation, Guangdong University of Technology. His research interests include the Internet of Things (IoT), the embedded applications, and the digital image processing.



MEHDI GHEISARI has published several papers in several domains with his colleagues in highly ranked journals, including *Computers and Security*, *Computer and Electrical Engineering*, *IEEE Access*, *IGRDJ*, *INDJST*, and in many highly ranked conferences, such as *IC3PP*, *CSCWD*, *ISPA*, *EUC*, and *ICAC*. He worked on WSN. His current research interest includes privacy preserving in the Internet of Things (IoT). His profile can be accessed via <https://scholar.google.com/citations?user=tmWQf9UAAA&hl=en>.



XIAOBO ZHANG was born in Suizhou, China, in 1977. He received the master's degree in computer science, and the D.Eng. degree in control theory and control engineering. He is currently with the Department of Automation, Guangdong University of Technology, where he is involved in the Internet of Things. He is also a Commissioner with Guangdong Science and Technology. He is also involved in teaching, technology research and development, product design, and scientific theoretical research in the field of industrial control and information technology services.

He has participated in more than 60 national and provincial research projects and corporate research projects, including the National Natural Science Foundations, the Natural Science Foundations of Guangdong Province, the major science and technology projects in Guangdong Province, and a combination of production, education, and research projects of the Ministry of Education of Guangdong Province. In recent years, there have been more than 30 papers published in academic journals with important influence at home and abroad, including three books as the Chief Editor. He has applied for more than 40 invention patents and obtained six software copyrights. His main research interests include hardware and software design for the Internet of Things (IoT) and big data, intelligent information processing and intelligent control (robot), and other industrial control systems.



GAUTAM SRIVASTAVA received the B.Sc. degree from Briar Cliff University, USA, in 2004, and the M.Sc. and Ph.D. degrees from the University of Victoria, Victoria, BC, Canada, in 2006 and 2011, respectively. He then taught for three years at the Department of Computer Science, University of Victoria, where he was regarded as one of the top undergraduate professors in the Computer Science Course Instruction. In 2014, he held a tenure-track position at Brandon University, Brandon, MB, Canada, where he is currently active in various professional and scholarly activities. He was promoted to Associate Professor, in 2018. In his eight-year academic career, he has published a total of 43 papers in high-impact conferences in many countries and in high-status journals, including *SCI* and *SCIE*, and has also delivered invited guest lectures on big data, cloud computing, the Internet of Things, and cryptography at many Taiwanese and Czech universities. As he is popularly known, he is active in research of data mining and big data. He has active research projects with other academics in Taiwan, Singapore, Canada, Czech Republic, Poland, and USA. He is constantly looking for collaboration opportunities with foreign professors and students Associate Professor. He received the Best Oral Presenter Award in *FSDM 2017*, which was held at the National Dong Hwa University (NDHU), Hualien, Taiwan, in 2017. He is an Editor of several international scientific research journals.

...